Heliyon 9 (2023) e22675

Contents lists available at ScienceDirect

Heliyon

journal homepage: www.cell.com/heliyon

Gold nanoparticles coated with PVP as a novel colorimetric sensor for sensitive and selective determination of Atenolol

Maryam Malmir, Farzaneh Shemirani *

Department of Chemistry, College of Science, University of Tehran, P.O. Box 14155–6455, Tehran, Iran

ARTICLE INFO

Keywords:
Gold nanoparticles
Polyvinylpyrrolidone
Colorimetric probe
Determination of atenolol
Aggregation
Hydrogen bonding

ABSTRACT

In this work, gold nanoparticles coated with polyvinylpyrrolidone (PVP-AuNPs) were used as a colorimetric probe for the sensitive, selective, simple, and rapid determination of atenolol (ATN). Indeed, atenolol triggered the aggregation of PVP-AuNPs via hydrogen bonding, electrostatic interactions, and dipole-dipole forces with PVP on the surface of AuNPs, causing the colloidal solution's color to shift from red to blue. SEM, TEM, FT-IR, UV–Vis, zeta potential, and other methods were used to characterise the PVP-AuNPs that were created as well as their aggregates. An excellent linear relationship between the absorption ratio (A690/A521) and the concentration of ATN in the range of 0.07–3.0 μM with a detection limit of 0.023 μM was discovered by optimising the experimental settings. The influence of potential interfering species on the measurement of ATN was investigated, and it was discovered that the developed colorimetric sensor had satisfactory selectivity. Finally, the presented method was used to measure ATN in tablet and blood plasma samples, and the obtained recovery values showed great promise for the use of the proposed sensor in clinical applications.

1. Introduction

Twenty-five percent of adults worldwide have hypertension or cardiovascular disease. As a result, β-blocker medications are increasingly being used to treat hypertension. Atenolol (ATN) is a β-blocker drug that is widely used to regulate blood pressure by blocking β_1 adrenergic receptors [1–3]. In addition, the use of this drug by athletes is considered doping because of its sedative properties [4,5]. Since the usage of ATEs is prohibited by the World Anti-Doping Agency (WADA), particularly for use by athletes in some sports, ATE-level monitoring is essential for drug abuse detection, particularly in athletes. In addition, level monitoring for patient dose management is of notable importance [6]. Atenolol is being used more often, which means that significant amounts of the drug and its metabolites may end up in surface water due to home sewage or wastewater treatment facilities. The examination of ATN is crucial for pharmacological and environmental studies because of its potential toxicity to aquatic organisms. The development of a quick screening technique to find its presence in pharmaceutical formulations and/or natural waters is therefore intriguing [7]. On the other hand, due to the narrow therapeutic window and significant toxicity of ATN at high dosages, monitoring this drug needs a sensitive and selective analytical method [8]. Due to their high sensitivity and selectivity, various chromatographic techniques have been used to measure ATN up until now [9]. However, despite the advantages mentioned, chromatography methods have limitations, such as the necessity for skilled and experienced operators, costly instrumentation, and special and expensive solvents. Apart from the aforementioned cases, another drawback of this method is the requirement for complicated sample pre-preparation processes that take

* Corresponding author.
E-mail address: fashemirani@ut.ac.ir (F. Shemirani).

https://doi.org/10.1016/j.heliyon.2023.e22675
Received 12 July 2023; Received in revised form 15 November 2023; Accepted 16 November 2023
Available online 22 November 2023

a lengthy time. While nanoparticle-based colorimetric sensors provide great accuracy and precision for measuring pharmaceuticals and chemicals, they are also considered simple and highly rapid techniques [10–12].

Due to their localised surface plasmon resonance (LSPR) characteristics, noble metal nanoparticles are now often used in optical sensors. For example, gold nanoparticles (AuNPs) are frequently used in colorimetric assays to determine a variety of analytes, including metal ions, macromolecules, and small molecules. This is because they have excellent chemical stability, a high extinction coefficient in the visible region of the spectrum, and an LSPR property in the visible region [13–17]. The LSPR characteristic of AuNPs has already been demonstrated to be affected by shape, size, nanoparticle environment, and inter-particle distance [18,19]. Therefore, when the distance between AuNPs decreases due to aggregation, a significant red shift occurs in their LSPR spectrum, which is the basis of colorimetric sensors [20–24]. On the other hand, modifying the surface of AuNPs to create aggregations in the presence of analytes is critical [25–27]. Hence, we modified the surface of AuNPs using polyvinylpyrrolidone (PVP) in order to develop a selective, sensitive, simple, and quick colorimetric sensor for the measurement of ATN (Fig. 1). In fact, atenolol promotes PVP-AuNPs to aggregate via hydrogen bonding, electrostatic interactions, and dipole-dipole interaction with PVP on the surface of AuNPs, which results in the colloidal solution shifting color from red to blue. The evaluation of the suggested sensor for detecting ATN in real samples demonstrates its high efficiency in pharmaceutical formulations, clinical, and hospital applications.

2. Materials and methods

2.1. Reagents and materials

Alfa Aesar® provided the hydrogen tetrachloroaurate (III) trihydrate ($HAuCl_4{\cdot}3H_2O$, 99.9 %). We supplied Atenolol and polyvinylpyrrolidone (PVP) with molecular weight ≈ 55,000 from Sigma-Aldrich®. Trisodium citrate dihydrate ($Na_3C_6H_5O_7{\cdot}2H_2O$), and other chemicals used were products of Merck® Company. We used deionized water (DI) with a resistivity of 18.2 MΩ cm and pH ≈ 6–7 to prepare our aqueous solutions.

2.2. Apparatus

An Agilent® 8453 spectrophotometer (USA) was utilized to collect absorption spectra. Using a field-emission microscope (TESCAN MIRA3 LMU, Czech Republic) running at an accelerating voltage of 15 kV, scanning electron microscopy (SEM) pictures were obtained. Using a Philipps EM 208 S microscope set to 100 kV, images from transmission electron microscopy (TEM) were captured. A PerkinElmer® (Model Spectrum GX) infrared spectrometer was used to do Fourier transform infrared (FTIR) analysis in the 4000-400 cm^{-1} wave region. The zeta potential of the particles measured using from a HORIBA® Nano Particle Analyzer SZ-100 (Japan). An elma-E−100-H – Elma Ultrasonic bath (Germany) and a Hettich®- UNIVERSAL 320 benchtop centrifuge (Germany) were used during experiments. A DanChrom® HPLC system (Kianshar Danesh Co., Iran) equipped with a multi-wavelength UV–Vis detector, along with clarity and compiler software was used for HPLC analysis.

2.3. Synthesis of AuNPs coated with PVP

Before synthesis, all glassware was washed in a bath of freshly made aqua regia (1:3 HNO_3/HCl) and completely rinsed with DI water. According to the literature, the AuNPs were synthesized by reducing $HAuCl_4$ with citrate [28]. First, a 100.0 mL two-neck flask was filled with a 1.0 mM $HAuCl_4$ solution, followed by a condenser in one neck and a stopper in the other. The flask containing the $HAuCl_4$ solution was then put in a 100 °C silicon oil bath to reflux under stirring conditions. The reaction solution was allowed to reflux for an additional 20 min after 10.0 mL of a 38.8 mM sodium citrate solution was added as soon as the reflux began (the solution's color has now changed from light yellow to deep red). The flask was removed from the bath and allowed to cool down to room temperature while being swirled. Finally, functionalized AuNPs with PVP were obtained using a ligand exchange reaction by adding 100.0 mg of PVP to the colloidal AuNPs solution while vigorously stirring and staying for 2 h under the same conditions for PVP to be placed on the surface of the AuNPs. Finally, the PVP-AuNPs were dispersed in DI water after the resulting colloidal solution was centrifuged three times at 12,000 rpm to eliminate any remaining PVP and citrate from the system.

2.4. Colorimetric detection of ATN using the PVP-AuNPs

For colorimetric detection of ATN, first 2.5 mL of colloidal solution PVP-AuNPs and different volumes of standard ATN solution

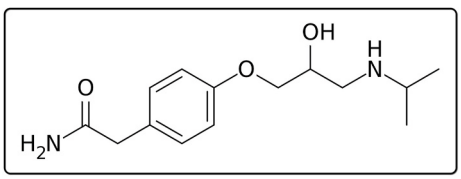

Fig. 1. Chemical structure of Atenolol.

were added to a series of 5.0 mL volumetric flasks, and then the flasks were filled with DI water up to the marked line. It should be mentioned that no buffer was needed because the pH of the deionized water used was between 6 and 7 (optimal pH). After thoroughly mixing the resulting solutions, their absorption spectra were immediately recorded using a UV–Vis spectrophotometer, and the analytical signal was defined as the absorption ratio (A_{690}/A_{521}).

2.5. Determination of ATN in real samples

The Iranian Blood Transfusion Organisation (IBTO) provided plasma samples, which were stored in a refrigerator before processing. The proteins were precipitated and separated from the samples by centrifuging the mixture for 20 min at 4000 rpm after thoroughly combining 0.2 mL of plasma samples with 1.6 mL of acetonitrile. The resultant supernatant was then diluted with DI water up to ten times. ATN was not found in plasma samples, thus different concentrations of ATN were added, and the recovery analysis was performed under the best lighting conditions with the colorimetric sensor that was planned. For the tablet samples' analysis, 10 tablets from the Sobhan Darou company (Iran, Tehran) with a label reading of 50.0 mg each were weighed, completely ground into powder, and then 100.0 mg of that powder was measured and added to 50.0 mL of DI water in a volumetric flask. Following that, it spent 30 min being sonicated in an ultrasonic bath. Following a 25-min centrifugation of the solution at 4000 rpm, the supernatant was filtered through ordinary filter paper. Finally, the recovery test was conducted using the suggested methodology. At the end of the process, the supernatants were collected and analyzed with high-performance liquid chromatography (HPLC) according to the United States Pharmacopeia (USP) monograph (Detection wavelength: 226 nm, Temperature: 25 °C, Column: C18, Flow rate: 0.6 mL/min, Injection size: 10 μL, Mobile phase: Sodium 1-heptansulfonate, Anhydrous dibasic sodium phosphate, and Dibutylamine).

3. Results and discussion

3.1. Characterization

As previously stated, surface modification of AuNPs is required to increase their selectivity for colorimetric sensors. Hence, to achieve this aim, AuNPs were functionalized with PVP for the determination of ATN. The successful synthesis of AuNPs coated with PVP was demonstrated using SEM, TEM, FT-IR, and UV–Visible spectroscopy techniques. The SEM and TEM images (Fig. 2a and b) show that spherical AuNPs with dimensions of around 13 nm and excellent monodispersity were successfully synthesized. The findings

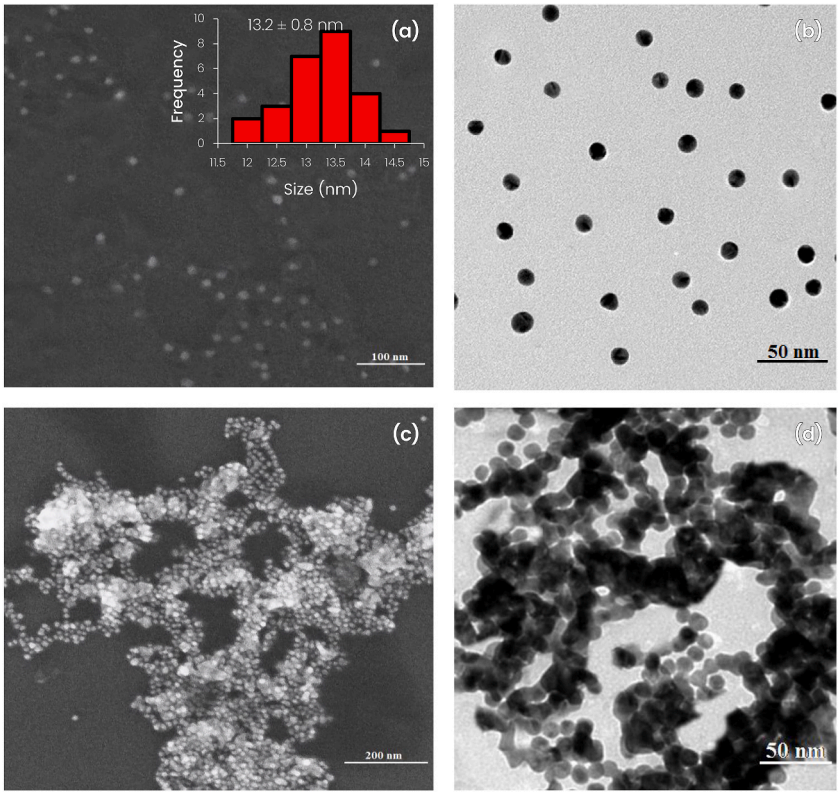

Fig. 2. SEM (a,c) and TEM (b,d) images of PVP-AuNPs in the absence (a,b) and presence (c,d) of ATN (the inset shows the size distribution of the PVP-AuNPs).

of the SEM and TEM images are confirmed by a narrow-width absorption peak at 521 nm in the UV–Vis spectrum (Fig. 3b). FT-IR spectroscopy was also employed to validate the surface modification of AuNPs with PVP. The FT-IR spectrum of PVP-AuNPs is depicted in Fig. 3a, and it is comparable to that of pure PVP. However, when compared to pure PVP, the CO stretch vibrational band exhibits a significant red-shift, which suggests that PVP is chemisorbed on the surface of AuNPs via the oxygen atom of its carbonyl group while the structure of PVP is left unaltered [29]. These findings demonstrate that the surface of AuNPs is completely coated with PVP.

3.2. Mechanism of ATN detection

The technique of atenolol measurement utilising PVP-AuNPs is depicted in Scheme 1. ATN colorimetric detection is based on the fact that PVP-AuNPs aggregate in the presence of atenolol, which causes a red-to-blue color change in the PVP-AuNPs solution. PVP is a solid dispersion excipient used in the pharmaceutical industry to increase the solubility and bioavailability of ATN. It has been shown that PVP interacts very strongly with ATN through hydrogen bonding and dipole-dipole forces [30,31], which are the crucial mechanisms of aggregation of PVP-AuNPs. Indeed, in aggregation, dipole-dipole interaction has occurred between –C═O of polymer (PVP) and –C═O of atenolol. Thus, in the proposed colorimetric sensor, PVP placed on the surface of AuNPs causes their aggregation via the mentioned interactions with ATN. In the first step, the UV–Visible spectroscopy technique was used to confirm these findings. As shown in Fig. 4, in the absence of atenolol, AuNPs exhibit an absorption peak at 521 nm; however, by introducing a certain amount of ATN, a new absorption peak at 690 nm appears, indicating the formation of AuNPs aggregation. In the meantime, it is easy to see how the color of the AuNPs solution changed from red to blue (see the inset of Fig. 4). In other words, the intensity of the absorption peaks at 521 and 690 nm is affected by the degree of dispersion and aggregation of AuNPs, respectively. Indeed, the value of (A_{690}/A_{521}) represents the ratio of aggregated to dispersed AuNPs. SEM and TEM images clearly show the formation of AuNPs aggregates and confirm the results obtained from UV–Visible spectra (Fig. 2c and d).

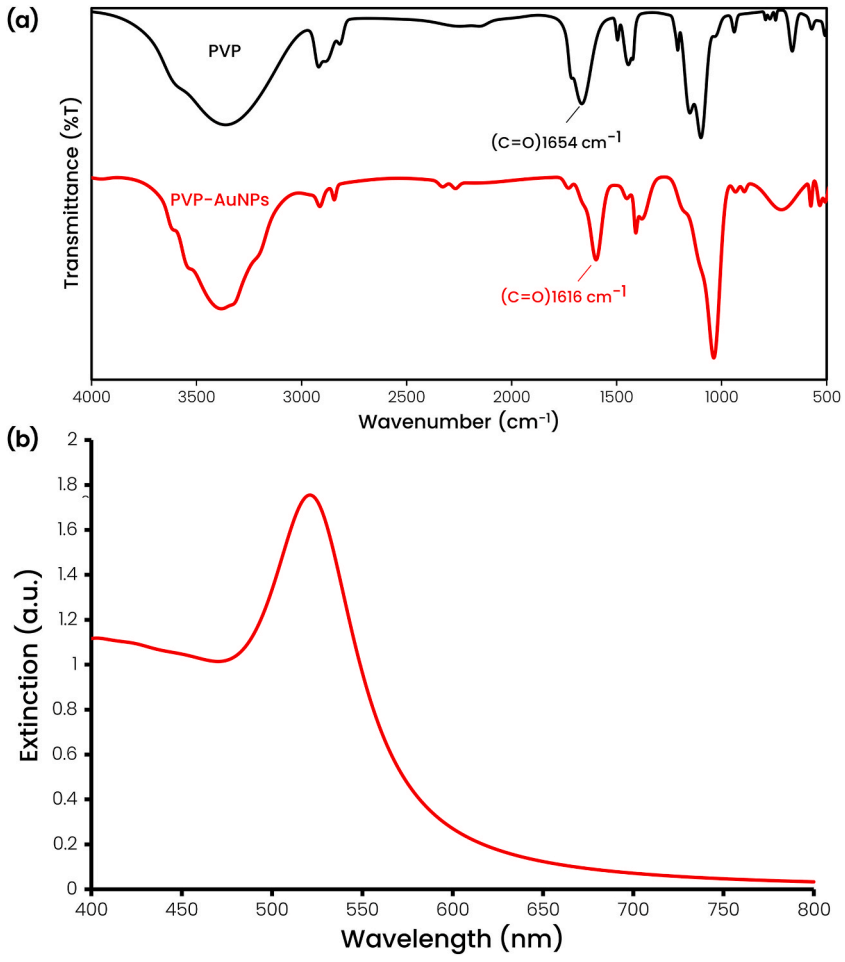

Fig. 3. a) FT-IR spectra of PVP and PVP-AuNPs. b) UV–Vis spectrum of PVP-AuNPs.

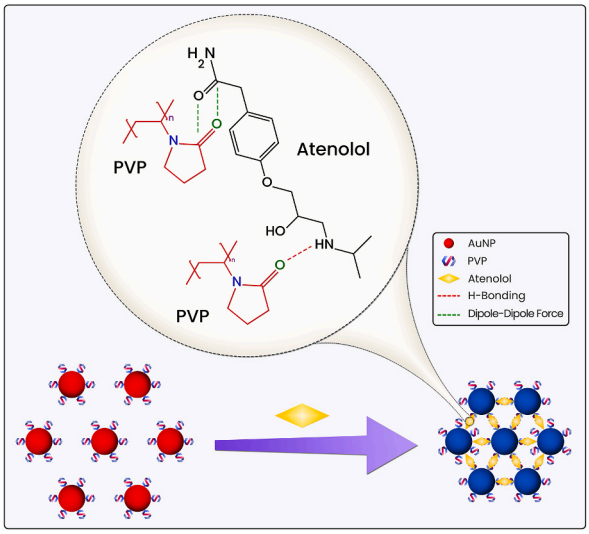

Scheme 1. General route for sensing ATN using the designed colorimetric sensor.

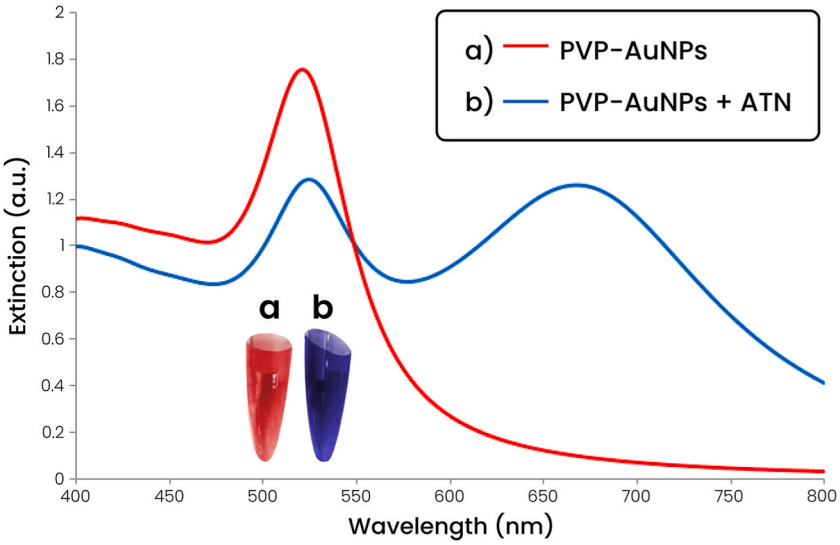

Fig. 4. UV–Vis spectra of PVP-AuNPs in the absence (a) and presence (b) of ATN (the inset shows changing color of PVP-AuNPs from red to blue after adding ATN).

3.3. Optimization of experimental conditions for ATN sensing

Since the physicochemical properties of the surfaces of AuNPs and ATN are pH- dependent, this parameter may affect the colorimetric sensor's response. Fig. 5a shows that the ratio of A_{690}/A_{521} is very low at the acidic pH, indicating that AuNPs aggregation does not occur. In the acidic pH range, ATN is protonated ($pK_a = 9.6$) and hence has a positive charge [32,33]. PVP, on the other hand, acts as a capping agent for AuNPs and, according to the results of zeta potential calculations, has a positive charge (Fig. 5c). Therefore, as electrostatic repulsion between charges are similar, the drug's electrostatic attraction to PVP precludes the formation of AuNPs aggregates at pH levels lower than 6. Due to the electrostatic attraction, hydrogen bonds, and dipole-dipole interaction between ATN and PVP-AuNPs, atenolol aggregates and changes the color of the solution from red to blue at pH 6–8, where atenolol still has a positive charge and PVP has a negative charge. In addition to dramatically lowering ATN's solubility under alkaline conditions, hydroxide ions also compete with the medication for surface adsorption and stop it from interacting with PVP-AuNPs.

The response time of the suggested colorimetric sensor was then studied. Because the interaction between PVP-AuNPs and ATN is very fast, the colorimetric sensor response remained constant from 0 to 15 min (Fig. 5b). As a result, absorption spectra were recorded immediately after adding ATN to AuNPs.

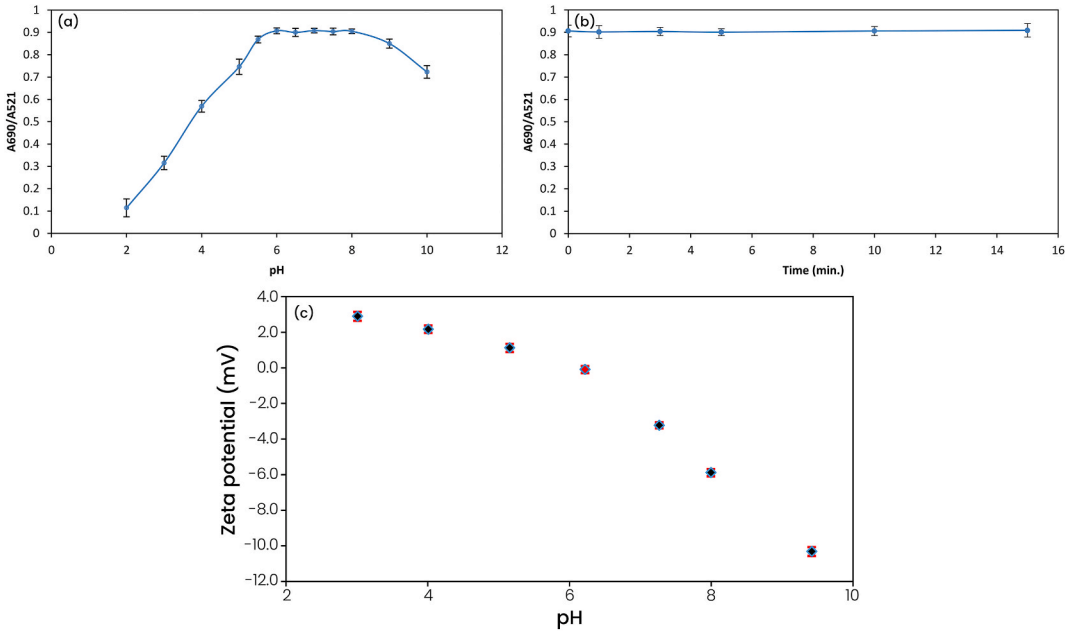

Fig. 5. a) Effect of pH on absorption ratio A690/A521 in presence of 2 μM ATN b) Effect of the incubation time on absorption ratio A690/A521 of the system with 2 μM ATN c) Zeta potential of PVP-AuNPs.

3.4. Selectivity

To evaluate the selectivity of the designed colorimetric sensor, 0.5 μM of ATN was determined under optimal conditions in the presence of possible interferents, including different ions (PO_4^{3-}, SO_4^{2-}, Mg^{2+}, Ca^{2+}, Na^{+}, K^{+}, Cl^{-}, and NO_3^{-}) and biological species (uric acid, urea, glucose, sucrose, fructose, lysine, and ascorbic acid). Since blood pressure-lowering medications are frequently taken in combination, the interfering effect of propranolol and metoprolol which are frequently administered with ATN was also investigated. The outcomes are displayed in Table 1. As can be seen, when the tolerance level of 5 % is taken into consideration, which is thought to be the greatest concentration of interferents causing a relative error of less than 5 % on the analyte response, the studied species show no interference on the atenolol assay.

To better show the selectivity for ATN, the colorimetric response in the presence of several interferences has been graphically demonstrated in Fig. 6. The suggested sensor has great selectivity and may be utilized to measure ATN in real samples with a complex matrix as a result of these findings.

Atenolol possesses two amino groups (-NH and $–NH_2$) and one hydroxyl group. These are the interactive sites in which hydrogen bindings with the synthesized nanoparticle occur and result in rapid aggregation. Other interferent molecules with amino or hydroxyl groups may interact with PVP-AuNPs but won't result in aggregation. One possible reason could be the presence of fewer amino groups in the interferent molecules (such as propranolol and metoprolol). Anther possible reason could be attributed to the limitation of stereo geometry of the moiety connected with the amino group in the interferent molecules.

3.5. Sensitive colorimetric determination of ATN

The absorption spectra of PVP-AuNPs (Fig. 7a) were recorded after introducing different concentrations of ATN under optimal conditions. Looking at Fig. 7, it is apparent that, as the concentration of atenolol increases, the intensity of the 521 nm peak decreases and a new peak appears at longer wavelengths, which gradually shows a significant red shift in addition to the increase in intensity,

Table 1
Interference effects of several coexisting substances for 0.50 μM of ATN.

Substance	MAC[a] (μM)	Calculated ATN[b] ($\overline{X} \pm$ SD)
Na^{+}, K^{+}, Ca^{2+}, Mg^{2+}, SO_4^{2-}, PO_4^{3-}, NO_3^{-}, Cl^{-}	10,000	0.487 ± 0.002
Glucose, Sucrose, Fructose, Ascorbic Acid, Lysine	5000	0.497 ± 0.001
Uric Acid, Urea	3000	0.503 ± 0.002
Propranolol	500	0.513 ± 0.001
Metoprolol	100	0.508 ± 0.003

[a] Maximum Allowable Concentration.
[b] Mean of three replicate analyses (n = 3).

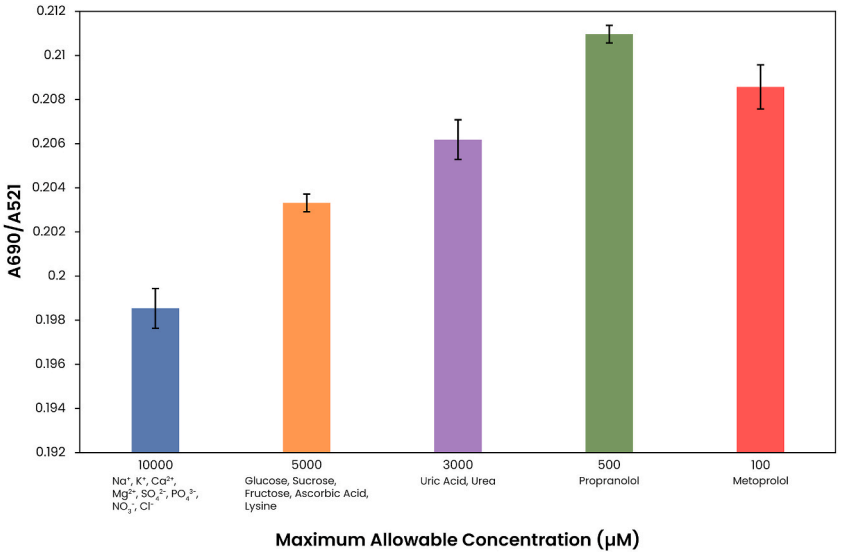

Fig. 6. Selectivity study of the colorimetric probe for ATN (Concentration of ATN: 0.5 μM).

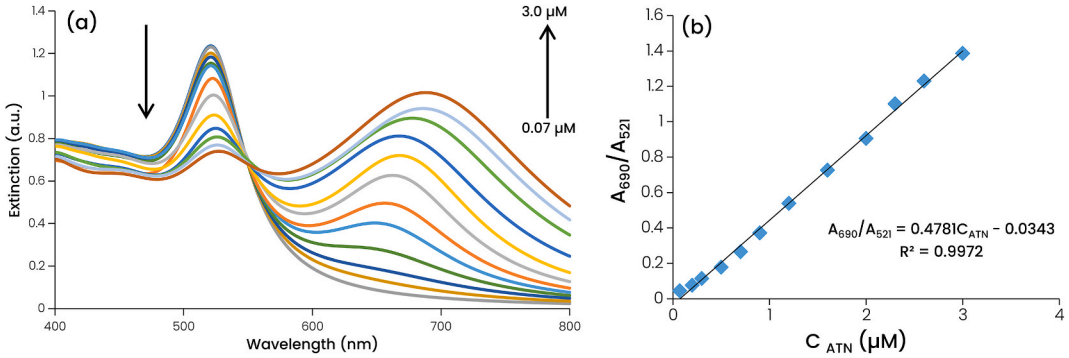

Fig. 7. a) UV–Vis spectra of the PVP-AuNPs in the presence of different amount of ATN (0.07–3.0 μM) b) Plot of the absorption ratio (A690/A521) vs. different concentrations of ATN.

Table 2
Comparison of the proposed method with alternate approaches for determination of ATN.

Analysis Method	LDR[a] (μM)	LOD (μM)	Ref.
LC-MS/MS[b]	0.0038–3.00	0.0038	[34]
MMIP-CE/DAD[c]	0.0188–5.63	0.0188	[35]
LC–HRMS[d]	0.0939–5.63	0.0939	[36]
UV–Vis	5.63–67.58	0.86	[37]
Fluorescence/QDs[e]/AuNPs	3.94–42.13	3.94	[38]
Electrochemical/PDA/GCE[f]	0.10–1.00	0.027	[39]
Electrochemical/DMZN/CPE[g]	0.11–125.87	0.010	[3]
Electrochemical/Lac/PAZ[h]-Bi_2Se_3 NPs/GCE	3.00–130.00	0.15	[1]
This work	0.07–3.00	0.023	–

[a] Linear dynamic range.
[b] Liquid chromatography-mass spectrometry/mass spectrometry.
[c] Magnetic molecularly imprinted polymer-capillary electrophoresis/diode array detection.
[d] Liquid chromatography–high resolution TOF mass spectrometry.
[e] Quantum dots.
[f] Poly-dopamine/glassy carbon electrode.
[g] $DyMnO_3$-ZnO nanocomposites/carbon paste electrode.
[h] Laccase/polyaziridine.

Table 3
Recovery of ATN (μM) in the blood plasma samples under optimum conditions (n = 3).

Sample	Colorimetric method				HPLC method		
	Added (μM)	Found (μM) ($\overline{X}$ ± SD)	Recovery %	RSD %	Found (μM) ($\overline{X}$ ± SD)	Recovery %	RSD %
Blood Plasma	0.000	N.D.[a]	–	–	–		
	0.100	0.101 ± 0.002	101.0	2.15	0.1005 ± 0.117	100.5	1.18
	0.500	0.494 ± 0.006	98.8	1.23	0.499 ± 0.005	99.8	1.10
	1.500	1.473 ± 0.011	98.2	0.75	1.486 ± 0.014	99.1	0.96
	2.000	2.016 ± 0.012	100.8	0.60	2.04 ± 0.025	101.2	1.25

[a] Not detected.

Table 4
Determination of ATN in commercial tablets (n = 3).

Sample	Colorimetric method				HPLC method		
	Added (mg)	Found (mg) ($\overline{X}$ ± SD)	Recovery %	RSD %	Found (mg) ($\overline{X}$ ± SD)	Recovery %	RSD %
Tablet (50 mg/tablet)	0.0	50.2 ± 1.079	100.4	2.15	49.75 ± 0.930	99.5	1.87
	25.0	74.8 ± 1.069	98.4	1.43	75.45 ± 1.177	100.6	1.56
	50.0	101.3 ± 0.861	102.2	0.85	101.8 ± 0.946	101.8	0.93

and eventually the position of the new peak at 690 nm remains constant. As a result, the calibration curve was created using changes in the absorbance ratio (A690/A521) that were proportional to the ATN concentration (Fig. 7b). The findings demonstrate a strong linear association (correlation coefficient of 0.9972) between the analytical signal value (A690/A521) and the concentration of ATN in the range of 0.07–3.0 μM. The signal-to-noise ratio (S/N = 3) was used to compute the limit of detection (LOD), and the result was 0.023 μM. Additionally, the outcomes of the proposed sensor's use were compared with those of alternative ATN measurement techniques. Table 2 shows that the suggested method outperforms most other methods in terms of sensitivity, linear range, and limit of detection.

3.6. Real sample analysis

ATN was evaluated in blood plasma and tablet samples to assess the practical application of this recently designed colorimetric sensor. The results are presented in Tables 3 and 4, and obtained were a mean of three replicate (n = 3). As can be identified, the recoveries fell between 98.2 and 102.2 %, with a relative standard deviation (RSD) of less than 2.15, demonstrating the proposed sensor's capability to detect ATN in human plasma and tablet samples. The sensor that was created is therefore appropriate for use in medical settings like hospitals. To evaluate the efficiency of our probe, the results of the colorimetric method have been compared to the results obtained from the HPLC method, which show virtually similar values.

4. Conclusion

In this investigation, AuNPs functionalized with PVP were employed as a colorimetric probe to carry out a quick, easy, sensitive, and specific detection of ATN. As a result of ATN's selective interaction with PVP via hydrogen bonds and dipole-dipole forces, AuNPs clump together and the colloidal solution's color shifts from red to blue. AuNPs functionalized with PVP were used in this study as a colorimetric probe to quickly, easily, sensitively, and precisely detect ATN. ATN selectively interacts with PVP through hydrogen bonds, electrostatic interactions and dipole-dipole forces, causing AuNPs to clump together and the color of the colloidal solution to change from red to blue. The LSPR peak exhibits a substantial red shift from 521 to 690 nm as well. With a detection limit of 0.023 μM, the absorbance ratio (A690/A521) was therefore chosen as the analytical signal, which was discovered to have a strong linear correlation with ATN concentrations ranging from 0.07 to 3.0 μM. Additionally, it was demonstrated that the colorimetric sensor that has been introduced offers a lot of potential for detecting ATN in biological and clinical samples through the examination of real samples.

Funding

This research did not receive any specific grant from funding agencies in the public, commercial, or not-for-profit sectors.

CRediT authorship contribution statement

Maryam Malmir: Writing – review & editing, Writing – original draft, Visualization, Validation, Software, Resources, Project administration, Methodology, Investigation, Formal analysis, Data curation. **Farzaneh Shemirani:** Supervision, Conceptualization.

Declaration of competing interest

The authors declare that they have no known competing financial interests or personal relationships that could have appeared to

influence the work reported in this paper.

Acknowledgements

I want to publicly thank *Dr. Farzaneh Shemirani*, my mentor and adviser at the University of Tehran, for all of her time, hard work, and patience in guiding me through my postgraduate studies.

I would like to thank *Dr. Amir Vasheghani-Farahani* from the bottom of my heart for his insightful criticism and literary contributions. He reviewed and edited the manuscript as well as visualized, including the finalization of all graphical materials.

I am also appreciative because the *University of Tehran's Faculty of Science* gave me the means to pursue graduate studies at the Chemistry Department.

Finally, I appreciate my family's support and affection for me because they always give me unconditional emotional support.

Appendix A. Supplementary data

Supplementary data to this article can be found online at https://doi.org/10.1016/j.heliyon.2023.e22675.

References

[1] A. Bathinapatla, G. Gorle, S. Kanchi, R.P. Puthalapattu, Y.C. Ling, An ultra-sensitive laccase/polyaziridine-bismuth selenide nanoplates modified GCE for detection of atenolol in pharmaceuticals and urine samples, Bioelectrochemistry 147 (2022), 108212, https://doi.org/10.1016/j.bioelechem.2022.108212.

[2] R.H. Patil, R.N. Hegde, S.T. Nandibewoor, Voltammetric oxidation and determination of atenolol using a carbon paste electrode, Ind. Eng. Chem. Res. 48 (23) (2009) 10206–10210, https://doi.org/10.1021/ie901163k.

[3] M. Valian, A. Khoobi, M. Salavati-Niasari, Green synthesis and characterization of DyMnO(3)-ZnO ceramic nanocomposites for the electrochemical ultratrace detection of atenolol, Mater. Sci. Eng., C 111 (2020), 110854, https://doi.org/10.1016/j.msec.2020.110854.

[4] R. Afonso, A.P.P. Eisele, J.A. Serafim, A.C. Lucilha, E.H. Duarte, C.R.T. Tarley, E.R. Sartori, L.H. Dall'Antonia, BiVO4–Bi2O3/ITO electrodes prepared by layer-by-layer: application in the determination of atenolol in pharmaceutical formulations and urine, J. Electroanal 765 (2016) 30–36, https://doi.org/10.1016/j.jelechem.2015.10.014.

[5] A. Khataee, R. Lotfi, A. Hasanzadeh, M. Iranifam, S.W. Joo, Flow-injection chemiluminescence analysis for sensitive determination of atenolol using cadmium sulfide quantum dots, Spectrochim. Acta: Mol. Biomol. Spectrosc. 157 (2016) 88–95, https://doi.org/10.1016/j.saa.2015.12.015.

[6] A.N. Hasanah, D. Rahayu, R. Pratiwi, T. Rostinawati, S. Megantara, F.A. Saputri, K.H. Puspanegara, Extraction of atenolol from spiked blood serum using a molecularly imprinted polymer sorbent obtained by precipitation polymerization, Heliyon 5 (4) (2019), e01533, https://doi.org/10.1016/j.heliyon.2019.e01533.

[7] C.M.F. Calixto, P. Cervini, É.T.G. Cavalheiro, Determination of atenolol in environmental water samples and pharmaceutical formulations at a graphite-epoxy composite electrode, Int. J. Environ. Anal. Chem. 92 (5) (2012) 561–570, https://doi.org/10.1080/03067310903582358.

[8] M. Arvand, M. Vejdani, M. Moghimi, Construction and performance characterization of an ion selective electrode for potentiometric determination of atenolol in pharmaceutical preparations, Desalination 225 (1–3) (2008) 176–184, https://doi.org/10.1016/j.desal.2007.06.017.

[9] V.-I. Iancu, G.-L. Radu, R. Scutariu, A new analytical method for the determination of beta-blockers and one metabolite in the influents and effluents of three urban wastewater treatment plants, Anal. Methods 11 (36) (2019) 4668–4680, https://doi.org/10.1039/c9ay01597c.

[10] G. Liu, M. Lu, X. Huang, T. Li, D. Xu, Application of gold-nanoparticle colorimetric sensing to rapid food safety screening, Sensors 18 (12) (2018), https://doi.org/10.3390/s18124166.

[11] M. Sabela, S. Balme, M. Bechelany, J.-M. Janot, K. Bisetty, A review of gold and silver nanoparticle-based colorimetric sensing assays, Adv. Eng. Mater. 19 (12) (2017), 1700270, https://doi.org/10.1002/adem.201700270.

[12] L. Zhang, J. Zhao, J. Jiang, R. Yu, Enzyme-regulated unmodified gold nanoparticle aggregation: a label free colorimetric assay for rapid and sensitive detection of adenosine deaminase activity and inhibition, Chem. Commun. 48 (89) (2012) 10996–10998, https://doi.org/10.1039/c2cc36240f.

[13] J. Mao, Y. Lu, N. Chang, J. Yang, S. Zhang, Y. Liu, Multidimensional colorimetric sensor array for discrimination of proteins, Biosens. Bioelectron. 86 (2016) 56–61, https://doi.org/10.1016/j.bios.2016.06.040.

[14] P.A. Rasheed, N. Sandhyarani, Electrochemical DNA sensors based on the use of gold nanoparticles: a review on recent developments, Microchim. Acta 184 (4) (2017) 981–1000, https://doi.org/10.1007/s00604-017-2143-1.

[15] P. Wang, Z. Lin, X. Su, Z. Tang, Application of Au based nanomaterials in analytical science, Nano Today 12 (2017) 64–97, https://doi.org/10.1016/j.nantod.2016.12.009.

[16] S. Wu, D. Li, J. Wang, Y. Zhao, S. Dong, X. Wang, Gold nanoparticles dissolution based colorimetric method for highly sensitive detection of organophosphate pesticides, Sensor. Actuator. B Chem. 238 (2017) 427–433, https://doi.org/10.1016/j.snb.2016.07.067.

[17] Y. Zhang, J. Jiang, M. Li, P. Gao, Y. Zhou, G. Zhang, S. Shuang, C. Dong, Colorimetric sensor for cysteine in human urine based on novel gold nanoparticles, Talanta 161 (2016) 520–527, https://doi.org/10.1016/j.talanta.2016.09.009.

[18] J.N. Anker, W.P. Hall, O. Lyandres, N.C. Shah, J. Zhao, R.P. Van Duyne, Biosensing with plasmonic nanosensors, Nat. Mater. 7 (6) (2008) 442–453, https://doi.org/10.1038/nmat2162.

[19] K.L. Kelly, E. Coronado, L.L. Zhao, G.C. Schatz, The optical properties of metal nanoparticles: the influence of size, shape, and dielectric environment, J. Phys. Chem. B 107 (3) (2002) 668–677, https://doi.org/10.1021/jp026731y.

[20] H. Chen, K. Zhou, G. Zhao, Gold nanoparticles: from synthesis, properties to their potential application as colorimetric sensors in food safety screening, Trends Food Sci 78 (2018) 83–94, https://doi.org/10.1016/j.tifs.2018.05.027.

[21] J.J. Feng, H. Guo, Y.F. Li, Y.H. Wang, W.Y. Chen, A.J. Wang, Single molecular functionalized gold nanoparticles for hydrogen-bonding recognition and colorimetric detection of dopamine with high sensitivity and selectivity, ACS Appl. Mater. Interfaces 5 (4) (2013) 1226–1231, https://doi.org/10.1021/am400402c.

[22] S.S. Memon, A. Nafady, A.R. Solangi, A.M. Al-Enizi, Shah M.R. Sirajuddin, S.T.H. Sherazi, S. Memon, M. Arain, M.I. Abro, M.I. Khattak, Sensitive and selective aggregation based colorimetric sensing of Fe3+ via interaction with acetyl salicylic acid derived gold nanoparticles, Sensor. Actuator. B Chem. 259 (2018) 1006–1012, https://doi.org/10.1016/j.snb.2017.12.162.

[23] C.L. Schofield, A.H. Haines, R.A. Field, D.A. Russell, Silver and gold glyconanoparticles for colorimetric bioassays, Langmuir 22 (15) (2006) 6707–6711, https://doi.org/10.1021/la060288r.

[24] Y. Yu, Y. Hong, Y. Wang, X. Sun, B. Liu, Mecaptosuccinic acid modified gold nanoparticles as colorimetric sensor for fast detection and simultaneous identification of Cr 3+, Sensor. Actuator. B Chem. 239 (2017) 865–873, https://doi.org/10.1016/j.snb.2016.08.043.

[25] G. De Luca, P. Bonaccorsi, V. Trovato, A. Mancuso, T. Papalia, A. Pistone, M.P. Casaletto, A. Mezzi, B. Brunetti, L. Minuti, A. Temperini, A. Barattucci, M. R. Plutino, Tripodal tris-disulfides as capping agents for a controlled mixed functionalization of gold nanoparticles, New J. Chem. 42 (20) (2018) 16436–16440, https://doi.org/10.1039/c8nj03086c.
[26] S. Melikishvili, I. Piovarci, T. Hianik, Advances in colorimetric assay based on AuNPs modified by proteins and, Nucleic Acid Aptamers. Chemosensors 9 (10) (2021) 281, https://doi.org/10.3390/chemosensors9100281.
[27] H. Zhang, Y. Qu, Y. Zhang, Y. Yan, H. Gao, Thioglycolic acid-modified AuNPs as a colorimetric sensor for the rapid determination of the pesticide chlorpyrifos, Anal. Methods 14 (20) (2022) 1996–2002, https://doi.org/10.1039/d2ay00237j.
[28] J. Liu, Y. Lu, Preparation of aptamer-linked gold nanoparticle purple aggregates for colorimetric sensing of analytes, Nat. Protoc. 1 (1) (2006) 246–252, https://doi.org/10.1038/nprot.2006.38.
[29] J. Xian, Q. Hua, Z. Jiang, Y. Ma, W. Huang, Size-dependent interaction of the poly(N-vinyl-2-pyrrolidone) capping ligand with Pd nanocrystals, Langmuir 28 (17) (2012) 6736–6741, https://doi.org/10.1021/la300786w.
[30] S.S. Bharate, S.B. Bharate, Bajaj A.N., incompatibilities of pharmaceutical excipients with active pharmaceutical ingredients: a comprehensive review, J. Excipients Food Chem. 1 (3) (2010) 1131.
[31] A. Marini, V. Berbenni, M. Pegoretti, G. Bruni, P. Cofrancesco, C. Sinistri, M. Villa, Drug-excipient compatibility studies by physico-chemical techniques; the case of Atenolol, J. Therm. Anal. Calorim. 73 (2) (2003) 547–561, https://doi.org/10.1023/a:1025478129417.
[32] A. Azais, J. Mendret, E. Petit, S. Brosillon, Evidence of solute-solute interactions and cake enhanced concentration polarization during removal of pharmaceuticals from urban wastewater by nanofiltration, Water Res. 104 (2016) 156–167, https://doi.org/10.1016/j.watres.2016.08.014.
[33] P.-H. Chang, W.-T. Jiang, B. Sarkar, W. Wang, Z. Li, The triple mechanisms of atenolol adsorption on Ca-montmorillonite: implication in pharmaceutical wastewater treatment, Materials 12 (18) (2019), https://doi.org/10.3390/ma12182858.
[34] E.M. Phyo Lwin, C. Gerber, Y. Song, C. Leggett, U. Ritchie, S. Turner, S. Garg, A new LC-MS/MS bioanalytical method for atenolol in human plasma and milk, Bioanalysis 9 (7) (2017) 517–530, https://doi.org/10.4155/bio-2016-0304.
[35] A.T.M. da Silva, B.C. Pires, L.A.F. Dinali, A.C.F.C. Maia, C.J. dos Santos, C. Sanches, W.d.S. Borges, K.B. Borges, Terephthalic acid-based magnetic molecularly imprinted polymer for enantioselective capillary electrophoresis determination of atenolol in human plasma, Sep. Purif. Technol. 261 (2021), 118257, https://doi.org/10.1016/j.seppur.2020.118257.
[36] G. Lawson, E. Cocks, S. Tanna, Quantitative determination of atenolol in dried blood spot samples by LC-HRMS: a potential method for assessing medication adherence, J. Chromatogr., B: Anal. Technol. Biomed. Life Sci. 897 (2012) 72–79, https://doi.org/10.1016/j.jchromb.2012.04.013.
[37] K.N. Prashanth, K. Basavaiah, Simple, sensitive and selective spectrophotometric methods for the determination of atenolol in pharmaceuticals through charge transfer complex formation reaction, Acta Pol. Pharm. 69 (2) (2012) 213–223.
[38] R.C. Castro, A.F.R. Lopes, J.X. Soares, D.S.M. Ribeiro, J.L.M. Santos, Determination of atenolol based on the reversion of the fluorescence resonance energy transfer between AgInS(2) quantum dots and Au nanoparticles, Analyst 146 (3) (2021) 1004–1015, https://doi.org/10.1039/d0an01874k.
[39] M. Amiri, E. Amali, A. Nematollahzadeh, Poly-dopamine thin film for voltammetric sensing of atenolol, Sensor. Actuator. B Chem. 216 (2015) 551–557, https://doi.org/10.1016/j.snb.2015.04.082.